QUARTERLY JOURNAL
OF THE
ROYAL METEOROLOGICAL SOCIETY

Vol. 126 APRIL 2000 Part B No. 565

Q. J. R. Meteorol. Soc. (2000), **126**, pp. 1219–1238

The vertical resolution sensitivity of simulated equilibrium temperature and water-vapour profiles

By ADRIAN. M. TOMPKINS[1]* and KERRY. A. EMANUEL[2]

[1]*Max Planck Institut für Meteorologie, Germany*
[2]*Massachusetts Institute of Technology, USA*

(Received 29 October 1998; revised 9 July 1999)

SUMMARY

Variability of atmospheric water vapour is the most important climate feedback in present climate models. Thus, it is of crucial importance to understand the sensitivity of water vapour to model attributes, such as physical parametrizations and resolution. Here we attempt to determine the minimum vertical resolution necessary for accurate prediction of water vapour.

To address this issue, we have run two single-column models to tropical radiative–convective equilibrium states and have examined the sensitivity of the equilibrium profiles to vertical resolution. Both column models produce reasonable equilibrium states of temperature and moisture.

Convergence of the profiles was achieved in both models using a uniform vertical resolution of around 25 hPa. Coarser resolution leads to significant errors in both the water vapour and temperature profiles, with a resolution of 100 hPa proving completely inadequate. However, fixing the boundary-layer resolution and altering only the free-tropospheric resolution significantly reduces sensitivity to vertical resolution in one of the column models, in both water and temperature, highlighting the importance of resolving boundary-layer processes. Additional experiments show that the height of the simulated tropopause is sensitive to upper-tropospheric vertical resolution.

At resolutions higher than 33 hPa, one of the models developed a high degree of vertical structure in the vapour profile, resulting directly from the complex array of microphysical processes included in the stratiform cloud parametrization, some of which were only resolved at high resolutions. This structure was completely absent at lower resolutions, casting some doubt on the approach of using relatively complicated cloud schemes at low vertical resolutions.

KEYWORDS: Convection Parametrization Radiative–convective equilibrium

1. INTRODUCTION

Atmospheric general-circulation models (GCMs) have been used extensively to investigate the possible climate change that could be induced by a climate forcing, such as increasing levels of atmospheric CO_2 (e.g. Senior and Mitchell 1993; Letreut *et al.* 1994; Mitchell *et al.* 1995; Murphy and Mitchell 1995). This involves many climate-system feedbacks which act to modify the basic climate response. The most important of these is the water-vapour feedback, in which a warmer atmosphere is expected to contain increased amounts of water vapour, a greenhouse gas.

In order to believe water-vapour predictions made by GCMs it is necessary to have confidence in the simulations of today's climate, and an important aspect of this is whether the vertical grids used are sufficient. Numerical convergence of the water-vapour profile with increasing vertical resolution would seem to be an essential criterion

* Corresponding author: Max Planck Institut für Meteorologie, Bundesstrasse 55, 20146 Hamburg, Germany. e-mail: Tompkins@dkrz.de

for determining whether to be able to trust model sensitivities in the vapour profile itself. Additionally, upper tropospheric errors, where resolution is often coarsest, are bound to affect other important GCM characteristics, such as cross-tropopause water-vapour transport, for example.

Recently, Emanuel and Zivkovic-Rothman (*1999*) questioned current vertical grids used in many GCM studies, pointing out that, since the scale-height for water vapour in the atmosphere is around 3 km, models require vertical resolutions somewhat finer than this to represent the water-vapour profile correctly. They found that degrading the vertical resolution of their column model from 25 to 100 hPa greatly reduced the sensitivity of the water-vapour profile to changes in the microphysical parametrization. For comparison, the widely used ECHAM4 GCM (Roeckner *et al.* 1996) uses 19 vertical layers in its standard format, with a resolution ranging from approximately 60 to 90 hPa in the mid to upper troposphere. Some recent climate-model investigations have used grids with 9 vertical levels (e.g. Hansen *et al.* 1997; Colman and McAvaney 1997), implying resolutions coarser than 100 hPa.

Coarse vertical resolution could result in excessive vertical diffusion of water vapour as a result of the implicit diffusion operating in the horizontal and, especially, the vertical advection schemes. There could also be problems related to specific physical processes. In the tropics, for example, deep convection is known to be the main source of water vapour (Betts 1990; Sun and Lindzen 1993; Liao and Rind 1997). The vapour profile is thus dependent on a myriad of cloud microphysical processes. Recognition of this has led to the development of both more complex stratiform cloud parametrizations for GCMs (e.g. Lohmann and Roeckner 1996; Fowler *et al.* 1996; Ghan *et al.* 1997), and increasingly advanced convective parametrizations (e.g. Emanuel 1991; Emanuel and Zivkovic-Rothman 1999), which attempt to represent the cloud microphysical processes that occur within the convective draughts themselves. The possible benefits of the increased sophistication of these schemes may not be realized if the vertical grid is too coarse to resolve the many processes that influence water vapour.

Limitations on computing resources obviously necessitate compromises in terms of resolution and complexity of parametrization schemes when operating any numerical model, especially when long integrations are required, as is often the case for climate models. There has been a tendency, however, to use increasing computing resources to improve horizontal resolution of climate models (e.g. Rind 1988; Sperber *et al.* 1994; Senior 1995; Williamson *et al.* 1995; Marshall *et al.* 1997), or to increase the complexity of subgrid-scale parametrizations, while relatively little attention has been paid to the effect of coarse vertical resolution. Lindzen and Fox-Rabinovitz (1989) pointed out that a vertical resolution should be selected that is dynamically commensurate with the horizontal resolution. This conclusion was supported by the experiments of Olga *et al.* (*1991*). Boville (*1991*) found that, with the exception of equatorial-wave behaviour, there was little sensitivity in the climate simulation to an increase of the vertical resolution from a grid size of 2.8 km to 0.7 km using a model with T21 horizontal resolution. Adequate simulation of equatorial waves was subsequently shown by Boville and Randel (1992) to require a resolution finer than 1 km in the vertical. These papers, thus, largely focused on the requirements for consistent large-scale dynamics. Additionally, Austin *et al.* (1997) found that increasing their GCM's vertical resolution from 19 to 49 levels, by adding the extra levels at or above the tropopause, greatly improved the simulated ozone distribution. In another paper, Colman and McAvaney (1997) examined the effect of increasing vertical resolution from 9 to 13 levels, using the extra levels to double the resolution in the upper troposphere and found, among other things, that the cloud feedback was actually of the opposite sign to that calculated in all

their other sensitivity tests, emphasizing that physical processes must be considered when selecting vertical resolution.

In this paper, we investigate the sensitivity of the simulated tropical water-vapour profile to vertical resolution by running two different models to radiative–convective equilibrium and examining the structure of the models' temperature and vapour profiles as well as their sensitivity to vertical resolution. In full global model simulations, the influence on water vapour of large-scale dynamics and the lack of steady equilibrium conditions renders the identification of resolution dependencies more difficult. Thus, the approach of using a column model is adopted, allowing an easy examination of the equilibrium state of the model's equations in the absence of large-scale dynamics. However, the removal of certain processes, such as horizontal and vertical advection, means that the investigation can only suggest a lower bound on the required vertical resolution.

2. COLUMN MODELS

In an initial attempt to verify that the conclusions are model independent, two column models were selected that contained different representations of convective and cloud microphysical processes. Both models contained convective and cloud microphysical parametrizations that have been extensively used in global-scale models.

(*a*) *ECHAM model*

The first model is the column version of the widely used ECHAM4 GCM (Roeckner *et al.* (1996); see also Chen and Roeckner (1996), Chen and Roeckner (1997), Lohmann and Feichter (1997), Manzini *et al.* (1997), Bacher *et al.* (1998), Moron *et al.* (1998)). The standard model uses a bulk mass-flux convective parametrization scheme based on that of Tiedtke (1989), containing separate representations of shallow and deep convection. An additional scheme accounts for convection originating above the boundary layer, but it was inoperative in the tropical scenario used here.

In preliminary investigations, it was found that the balance between the shallow and deep convective parametrizations was sensitive to vertical resolution, also affecting the water-vapour profiles, and thus only the deep convective scheme was used in the investigations contained in this paper. This emphasizes the crucial importance of controlled tests in evaluating individual components of large and complicated models. Large-scale dynamics in global simulations can obscure model deficiencies which are immediately apparent when simple equilibrium tests are conducted. Thus, although global simulations obviously play an important role in the investigation and evaluation of new components of large-scale models, long timescale equilibrium tests, examining the equilibrium profiles of model variables such as water vapour, should also be conducted, as advocated previously by Emanuel (1994) and Emanuel and Zivkovic-Rothman (1999).

The deep convection scheme is modified according to Nordeng (1994) to make cloud-base mass flux a function of the convective available potential energy (CAPE), and with buoyancy-dependent entrainment and detrainment. Microphysical processes within convective updraughts themselves are crudely considered by raining out a height-dependent proportion of the in-draught condensate. Liquid water and ice detrained from convection are treated as a source for the stratiform cloud scheme, which includes a prognostic treatment of ice cloud and representations of many ice and liquid cloud microphysical processes (Lohmann and Roeckner 1996).

Surface fluxes of heat and moisture are calculated using Monin–Obukhov similarity theory. The turbulent transfer of heat, momentum, moisture and cloud water is incorporated using a first-order closure scheme.

(*b*) *Emanuel model*

In an attempt to verify the results obtained from the ECHAM model, we employed a second column model based on the convective scheme of Emanuel (1991) and Emanuel and Zivkovic-Rothman (1999). This convective scheme differs from the bulk mass-flux scheme of ECHAM in that it attempts to incorporate physical representations of the inhomogeneous mixing and associated microphysical processes that have been shown to occur in cumulus clouds. Convective heat and moisture transfer is accomplished by an ensemble of sub cloud-scale elements that undergo mixing with environmental air to varying degrees, based on the episodic model of Raymond and Blyth (1986). The associated microphysical processes in draughts permit the autoconversion of a certain proportion of cloud water to precipitation, with the threshold altered above the freezing level to account crudely for ice processes.

Thus, one important difference between the models is that the ECHAM model places emphasis on a fairly complex stratiform cloud scheme but uses a simple representation of microphysics in convective draughts, while the Emanuel model tries to represent the complex interaction between convective draughts and microphysics, but neglects many of the other cloud processes included in ECHAM stratiform scheme and does not predict stratiform cloud cover.

However, while stratiform cloud processes are not explicitly included in the Emanuel scheme, the parameters governing the formation, fall and re-evaporation of precipitation have been extensively tuned by Emanuel and Zivkovic-Rothman (1999) to achieve accurate predictions of relative humidity using data from the Intensive Flux Array (IFA) operated during TOGA–COARE*. Stratiform cloud processes are thus implicitly taken into account in as much as they affect the observed relative humidity in the IFA. The scheme also includes a hydrostatic, unsaturated downdraft driven by evaporation of precipitation. Independent tests (i.e. without additional tuning) using GATE† data were reasonably successful in predicting relative humidity.

3. SET-UP

The experiments were designed to mimic the simple tropical set-up used for the radiative–convective equilibrium investigations of Tompkins and Craig (1998a) and Tompkins and Craig (1999). Therefore, the forcing for convection is provided solely via radiative cooling of the atmosphere and surface fluxes of heat and moisture provided from an underlying ocean having a fixed temperature of 300 K. In the surface flux scheme of ECHAM, a surface velocity of 10 m s^{-1} is assumed, whereas the Emanuel model uses a lower surface velocity of 7 m s^{-1}, which is enhanced by a surface wind 'gust factor' related to the current downdraught mass flux.

Radiative cooling rates in the Emanuel model are provided by a radiation scheme described in Chou *et al.* (1991), that takes temperature and water vapour into account. Since the model currently does not estimate cloud fraction, cloud–radiation interactions are ignored and the radiative cooling rates are simply updated every 24 hours. The ECHAM model also has a radiation scheme available, but preliminary investigations showed that the diagnostic method of calculating cloud fractions, based solely on relative humidity, produces very high cloud fractions in the upper troposphere as the layer tends towards saturation (as it is constrained to do in most current column models).

* Tropical Ocean/Global Atmosphere Coupled Ocean–Atmosphere Response Experiment—a component of the World Climate Research Programme.

† GARP (Global Atmospheric Research Programme) Atlantic Tropical Experiment.

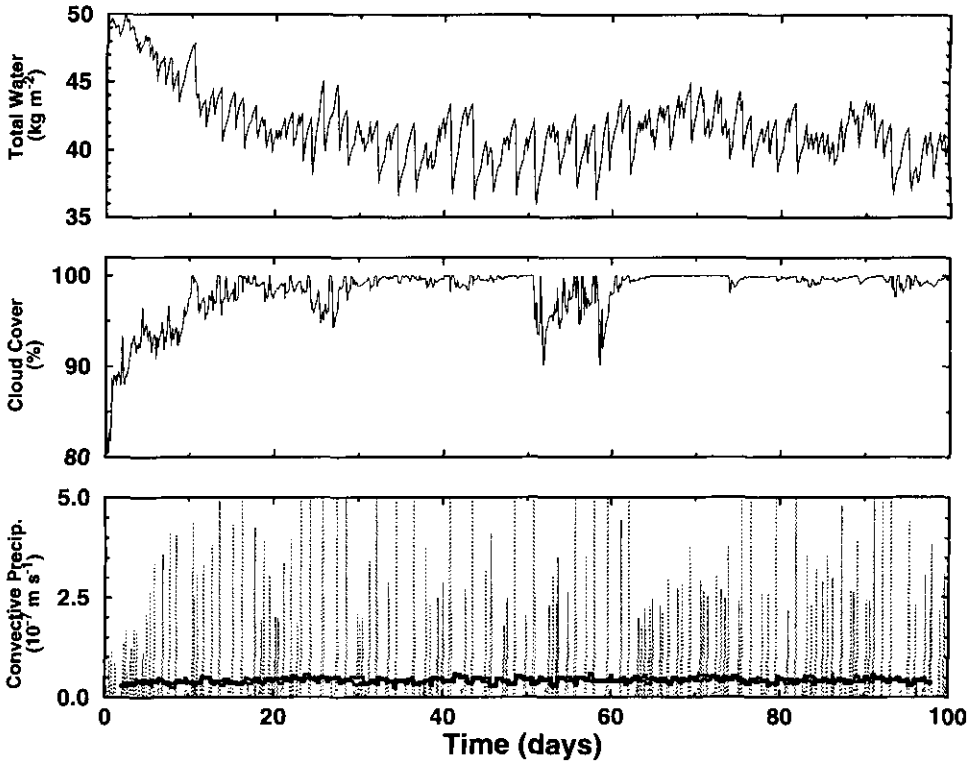

Figure 1. Time-series of convective precipitation, total cloud fraction and total column water vapour for the ECHAM column model using the standard 19 vertical-layer grid. The thick line on the convective precipitation graph represents a 50 point running average.

This induces a strong feedback between convection and radiation and produces large oscillations in the model fields, making the determination of the equilibrium state more difficult. Thus, for this initial simple investigation, the mean equilibrium radiative cooling rates of the control run of Tompkins and Craig (1999), linearly interpolated onto the column-model grid, were used in the ECHAM model. The models were integrated for a period of 100 days, since nearly 30 days (the radiative–subsidence timescale) are required for equilibrium to be reached (Tompkins and Craig 1998b). The time step used for the ECHAM model was 20 min, whereas the Emanuel model used 10 min.

For the basic runs shown in the next section, the ECHAM model used its standard 19-layer grid which has high resolution in the boundary layer. The Emanuel model had a grid spacing that was uniform in pressure from the surface to 100 hPa, with a resolution of $\Delta\sigma = 0.05$, with 10 extra levels placed above this, as required for the radiation scheme (see Table 1 for details)*.

4. Equilibrium description

(a) *Approach to equilibrium*

To demonstrate the adjustment to equilibrium, Fig. 1 shows time-series of total column water vapour, cloud cover and convective precipitation for ECHAM. Instantaneous values sampled at 2-hour intervals are shown. Two distinct timescales of adjustment can

* $\sigma = p/p_s$, where p is the pressure and p_s is the pressure at the earth's surface.

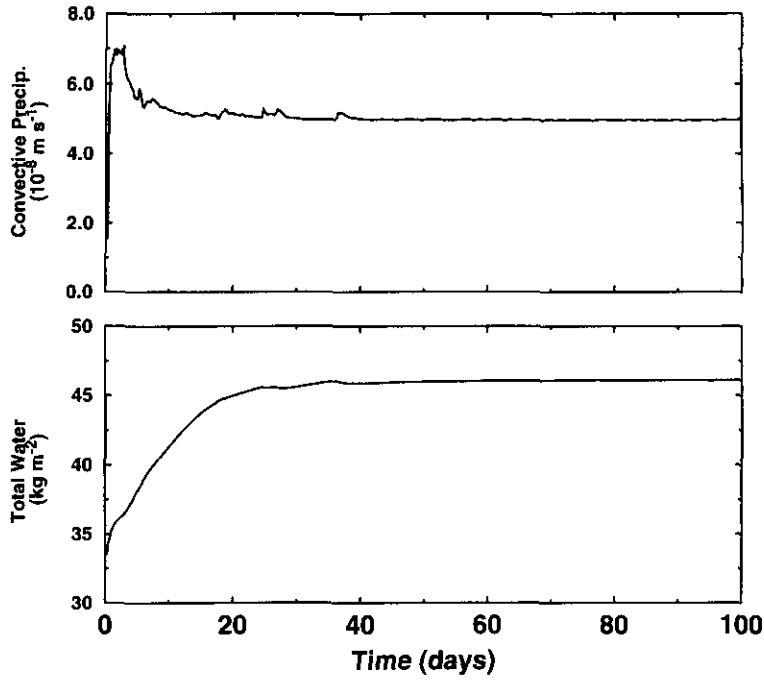

Figure 2. Time-series of precipitation and total column water vapour for the EMANUEL column model using 20 vertical layers.

be seen. The convective precipitation adjusts quickly to it's equilibrium state with high short-term variability. It is tempting, but incorrect, to associate the variability produced by such column models with the variability in rainfall one would expect at a specific location (i.e. representing a single grid point of a GCM). The forcing for the convection is unchanging in time and, therefore, cannot provide a mechanism for variability. There will also, of course, be stochastic variability in the activity of a large ensemble of cumulus clouds that the column model should in principle represent. But the convective scheme, like all others currently in use, does nothing to estimate this stochastic variability. The variability in ECHAM is therefore artificial, and indicates that the parametrized vertical mass-flux profile is unable to adapt fully to the forcing profile. Instead of exactly balancing the forcing each time step, the convective scheme can only achieve this balance over many time steps. Representing the variability of convection correctly is an important issue, since this can affect the whole variability of tropical atmospheric dynamics and can also influence the way convection and large-scale atmospheric waves interact (Slingo *et al.* 1994; Brown and Bretherton 1995).

The second timescale is clearly seen in the trend of the total water vapour, which exhibits a long adjustment, with equilibrium status obtained after approximately 30 days of integration. This long timescale adjustment is related to the time required by air to subside through the clear-air environment surrounding convection, which is directly related to the radiative cooling rate. This adjustment process operates on a local cumulus scale, in addition to the wider Hadley circulation scales (Tompkins and Craig 1998b), and, therefore, is only represented in mass-flux schemes such as used here. The final equilibrium value of the total column vapour is 41 kg m^{-2}. This falls at the lower end of observational values obtained from various satellite and sonde data sources, which generally range from 40 to 45 kg m^{-2} for this sea surface temperature (SST) (Prabhakara

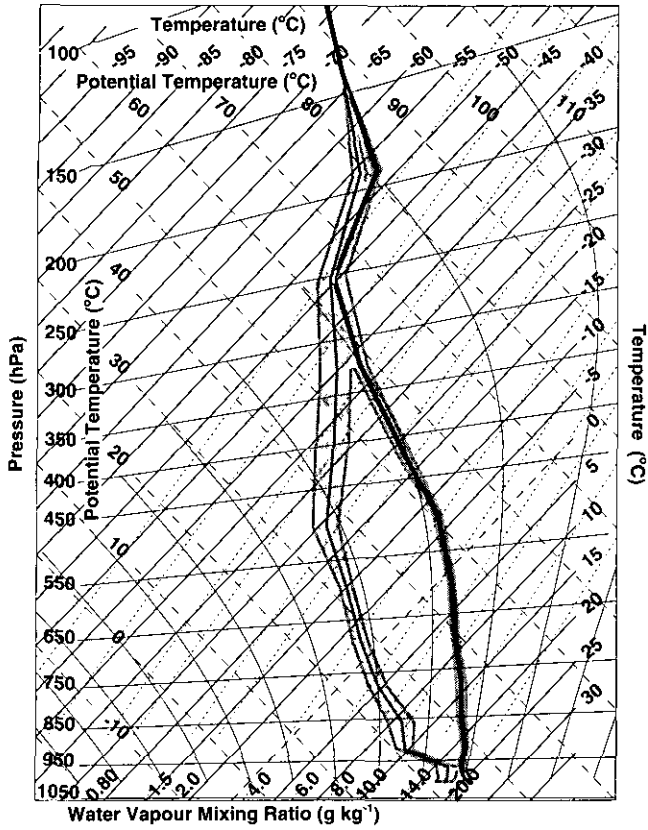

Figure 3. Tephigram plotting equilibrium temperature (thick solid line) and dew point (thin solid line) for the ECHAM (19 layer) model. The shaded area to each side of the temperature and dew-point curves mark one standard deviation to indicate temporal variability. The tephigram lines show temperature (solid diagonal lines labelled top and right in °C), potential temperature (long dashed diagonal lines labelled inside top and left in °C), pressure (solid horizontal lines labelled outside left in hPa) and water-vapour mixing ratio (short dashed lines labelled bottom in g kg^{-1}). The three unlabelled water-vapour lines represent mixing ratios of 0.15, 0.3 and 0.6 g kg^{-1} respectively. The curved solid lines indicate moist adiabats (not labelled).

et al. 1985; Stephens 1990; Gaffen *et al.* 1992; Raval *et al.* 1994; Weaver *et al.* 1994). This contrasts with the behaviour of the full ECHAM GCM, using the standard convective parametrization implementation, which generally produces higher amounts of total column vapour in the equatorial oceanic regions subject to deep convection (Chen *et al.* 1996).

In contrast to the ECHAM model, the time-series of precipitation and total column water vapour in Fig. 2 reveals little short timescale variability in the Emanuel model and, once the scheme settles into its equilibrium state, the model fields remain constant. Since the radiative cooling rates derived from the interactive scheme are similar to those imposed on the ECHAM model, the timescale for equilibrium to be achieved is again approximately 30 days. The equilibrium value of total column water vapour at approximately 46 kg m^{-2} is higher, but again very close to observations.

(*b*) *Equilibrium statistics*

Figure 3 shows a tephigram of the ECHAM's equilibrium state. The average values of temperature and dew-point between day 40 and 100 of the integration are plotted.

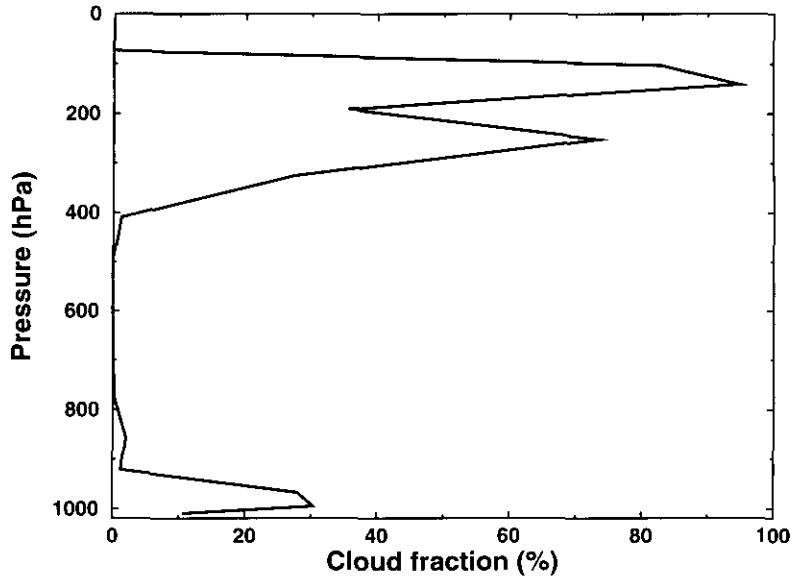

Figure 4. Cloud fraction profile as a function of pressure for the equilibrium of the 19-layer ECHAM model.

A number of characteristics can be observed in the plot. The boundary layer is dry adiabatic, with water vapour well mixed, and is 590 m deep. The temperature profile is roughly moist adiabatic, but the entrainment of environmental air, which is assumed to be homogeneously mixed through the convecting plume, produces a cooler upper troposphere than would be produced by an unmixed parcel ascent. The model seems to produce a very low tropopause, with the temperature lapse rate decreasing sharply at the 250 hPa level. Above the boundary layer, the moisture drops significantly, with a relatively dry lower troposphere in evidence. The tephigram uses ice saturation mixing ratios above the freezing point and so the graph shows that the 250 hPa level is almost saturated with respect to ice. This is the height to which most deep convection reaches.

The time-series of cloud fraction (Fig. 1) reveals that the total cloud fraction approaches unity almost immediately after the start of the integration. This directly reflects the 100% cloud fraction at the deep-convection detrainment levels, shown in Fig. 4. The limited magnitude of the convective forcing, consisting of a standard tropical radiative cooling profile with no large-scale forcing, is consistent with a scenario of scattered deep convection in the mid or west Pacific and, thus, such high cloud fractions are perhaps unexpected. A peak in cloud fraction is also visible associated with shallow convective overturning in the boundary layer.

In contrast to ECHAM, Fig. 5 shows that the Emanuel column model produces a much warmer equilibrium state, with an associated moister and smoother vapour profile. The Emanuel model also saturates the upper troposphere, and has a well represented boundary layer. In the vapour profile a clear dipole structure is produced, with the demarcation between the upper and lower parts clearly determined by whether ice or warm-rain physics operate. The small kink in the temperature profile reflects the effects of the change in fall speed of precipitation across that level The drop in water vapour above the boundary layer is quite substantial, with the mixing ratio dropping to around 10 g kg^{-1} at 850 hPa.

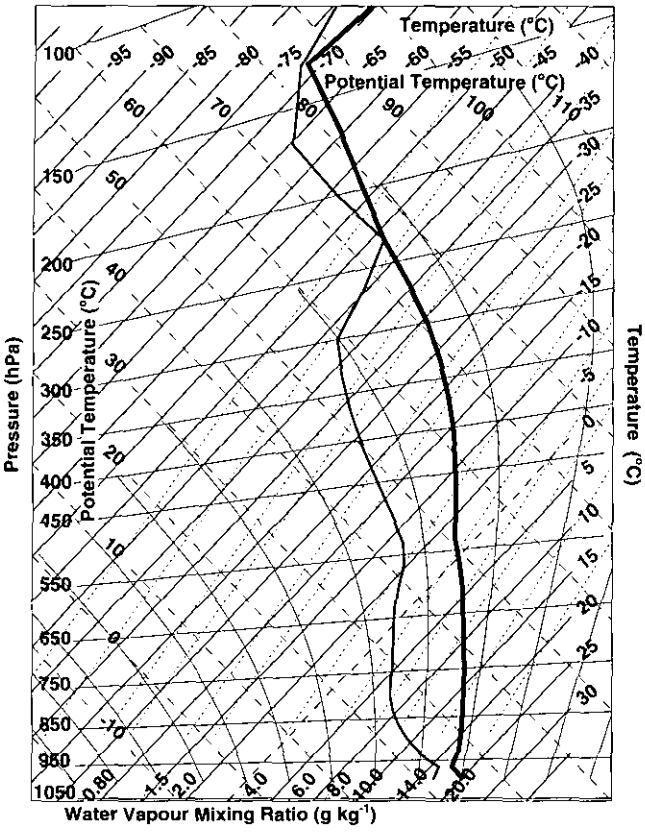

Figure 5. Tephigram plotting equilibrium temperature (thick line) and dew point (thin line) for the Emanuel model using a $\Delta\sigma = 0.05$ ($\approx$50 hPa) tropospheric resolution.

Since the water-vapour structure is one of the most difficult aspects for a model to predict, Fig. 6 compares the equilibrium relative-humidity profiles of the two column models with the profiles in the control-run equilibrium state of the cloud-resolving model (CRM) study of Tompkins and Craig (1999), which uses an identical fixed SST, no large-scale forcing, and which also provided the radiative cooling rates used to force the ECHAM model. (Note, however, that the Emanuel model uses a separately calculated radiative cooling profile.)

The ECHAM model produces a equilibrium atmospheric state with lower relative humidities throughout the troposphere to 400 hPa. The possible reasons for this are numerous, but are likely to be of microphysical origin, since the forcing for convection in ECHAM is taken from the CRM. Simply converting less cloud into rain within the convective updraughts would increase relative humidities, as would increasing rain (snow) evaporation (sublimation) rates. For example, decreasing the conversion of cloud into rain in convective updraughts by a factor of two in the ECHAM model increases relative humidities by up to 20% uniformly between 800 hPa and 300 hPa, making them more comparable to those of the CRM study (not shown). The sensitivity of water vapour to cloud microphysics was explored extensively by Rennó *et al.* (1994). With the Emanuel model, the contrast between the treatment of ice and warm-phase microphysics is highlighted, for example the assumed fall speed of condensates, with the upper troposphere having a higher relative humidity than in the CRM, and the reverse

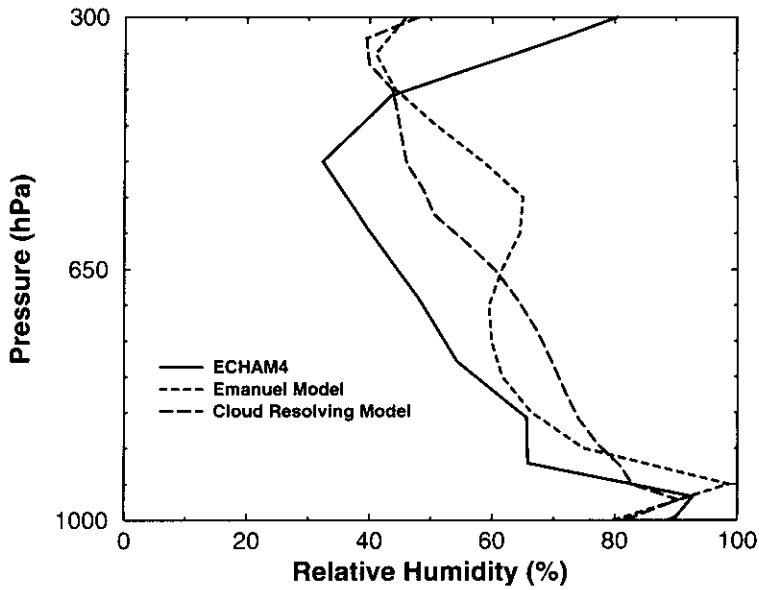

Figure 6. Equilibrium relative humidity (with respect to ice above the freezing level) for the ECHAM (19 layer) and Emanuel (50 hPa) models. For comparison, the equilibrium relative humidity from the cloud-resolving-model study by Tompkins and Craig (1999) is shown.

occurring in the lower troposphere. When comparing the column models with the CRM, it should be kept in mind that the CRM, although explicitly resolving cloud motions, still includes parametrizations for relatively unknown microphysical processes, and does not therefore necessarily represent 'reality'.

5. Vertical-resolution sensitivity

Here the basic sensitivity of the equilibria to vertical resolution is examined. Three series of experiments were conducted with the ECHAM model. In the first set of experiments, the atmosphere was simply divided into equal pressure layers, with the number of layers increased until numerical convergence was achieved.

Since the resolution of the atmospheric boundary layer is usually considered important, with models often utilizing an increased resolution there, a second set of experiments was conducted with the resolution held constant in the boundary layer. A third set of experiments then investigated the role of the vertical resolution in the deep-convective detrainment zone by additionally fixing the resolution above 300 hPa, and only increasing the mid-tropospheric resolution.

The resolution sensitivity of the Emanuel model is also examined, with the number of equal thickness layers between the surface and 100 hPa increased, but with the 10 layers above 100 hPa remaining fixed, as given in Table 1. The grids used are summarized in Table 2.

(*a*) *ECHAM*

Given the reasonable equilibrium profiles produced by ECHAM in its standard configuration, Fig. 7 reveals a significant response to increasing vertical resolution. Examining first the temperature, it is seen that, excluding the 10-level case, increasing vertical

TABLE 1. VERTICAL GRIDS OF THE ECHAM AND EMANUEL MODELS (IN σ COORDINATES) FOR THE CONTROL EXPERIMENTS

ECHAM model	Emanuel model
0.000	0.005
0.020	0.010
0.039	0.015
0.060	0.020
0.085	0.025
0.118	0.030
0.161	0.040
0.216	0.060
0.282	0.080
0.360	0.100
0.447	.
0.540	.
0.634	.
0.726	Resolution of
0.810	$\Delta\sigma = 0.05$
0.882	.
0.936	.
0.973	.
0.992	.
1.000	1.000

TABLE 2. DETAILS OF THE VERTICAL-RESOLUTION SENSITIVITY EXPERIMENTS

Experiment	Number of layers	Equivalent resolution
ECHAM (uniform resolution)	10, 20, 30, 40, 50	$\Delta\sigma = 0.1, 0.05, 0.033, 0.025, 0.02$
ECHAM (fixed boundary layer)	23, 32, 41, 50	$\Delta\sigma = 0.02$ between $\sigma = 0.9$ and $\sigma = 1.0$ $\Delta\sigma = 0.05, 0.033, 0.025, 0.02$ otherwise
ECHAM (fixed boundary layer and tropopause)	32, 38, 44, 50	$\Delta\sigma = 0.02$ between $\sigma = 0.9$ and $\sigma = 1.0$ and between $\sigma = 0.3$ and $\sigma = 0.0$ $\Delta\sigma = 0.05, 0.033, 0.025, 0.02$ otherwise
EMANUEL (uniform resolution)	28, 37, 46, 55, 70	$\Delta\sigma = 0.05, 0.033, 0.025, 0.02, 0.15$ 10 layers above $\sigma = 0.1$ (see Table 1)

resolution produces a trend towards a cooler atmosphere, with upper tropospheric differences amounting to a maximum of around 5 K, but with significant differences visible throughout the troposphere. With just 10 layers ($\approx$100 hPa), the model produces an uneven temperature profile, with large temperature deficits near the tropopause.

The differences in the water-vapour profile are more distinct, with a large degree of structure becoming apparent as resolution is increased. Convergence is achieved, for both temperature and moisture, with 40 vertical layers; equivalent to a layer depth of approximately 25 hPa. The profiles for 50 layers are exactly reproduced when 60 and 70 layers are used (not shown). In terms of total water vapour, there is very little sensitivity to resolution, owing to that fact that the greatest changes are restricted to the upper part of the troposphere.

In order to highlight the difference that vertical resolution can make, Fig. 8 compares the 50-layer converged equilibrium temperature and moisture profiles with those obtained using the standard 19-layer grid that was used almost exclusively in previous ECHAM investigations. Not only is the vertical variation in temperature and moisture

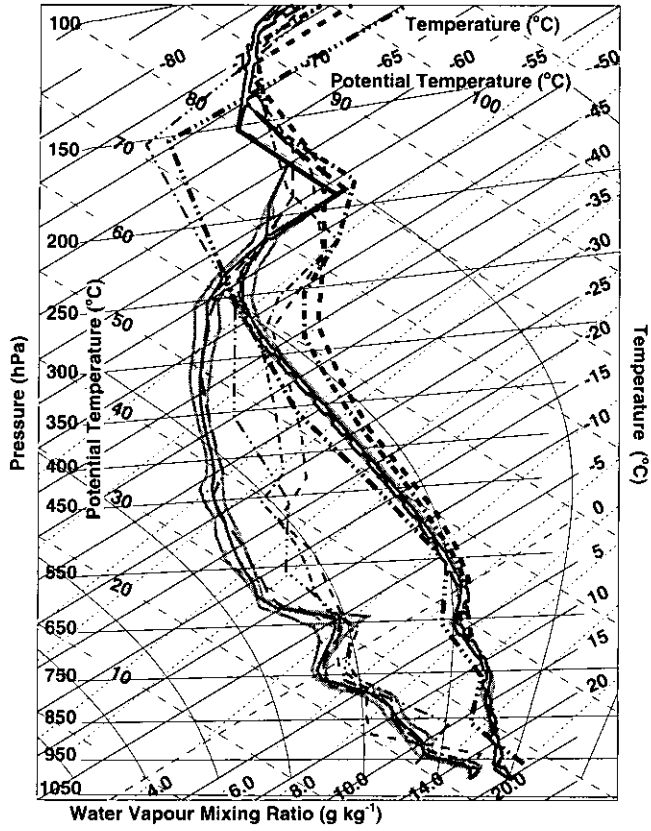

Figure 7. Tephigram plotting equilibrium temperature (thick lines on right, as in Fig. 3) and dew point (thin lines) for the ECHAM model using a resolution of $\Delta\sigma = 0.1$ (dot-dot-dashed lines), $\Delta\sigma = 0.05$ (dashed lines), $\Delta\sigma = 0.033$ (dot-dashed lines), $\Delta\sigma = 0.025$ (long dashed lines), $\Delta\sigma = 0.02$ (solid lines). The shaded area indicates the standard deviation of the $\Delta\sigma = 0.02$ case. This and subsequent tephigrams are plotted using a sub-region of Fig. 3 to enable the differences to be more clearly seen.

highly smoothed when using the standard grid, but large absolute differences in temperature and moisture exist, particularly in the upper troposphere. At 325 hPa, for example, the standard grid produces a mean water-vapour mixing ratio of 0.41 g kg^{-1}, nearly twice that of the converged value of 0.23 g kg^{-1}. This comparison also reveals a deficiency in the model's simulation of the atmosphere above the tropopause. With the standard 19-level grid, the temperature profile already exhibited a significant increase in lapse rate above 200 hPa, but with high vertical resolution the layer between 200 and 150 hPa becomes dry adiabatic. This is another feature of the inability of the model's mass flux to adapt to the imposed forcing, which also caused the short timescale variability in the equilibrium state.

By fixing the levels in the boundary layer, the sensitivity of ECHAM to vertical resolution is reduced (Fig. 9), particularly in the temperature profile. This reveals the importance of resolving the boundary layer, justifying the choice of increased boundary-layer resolution commonly applied. Using a coarser resolution in the boundary layer affects the calculation of the lifting condensation level for convection and the subsequent moist adiabat and water content adopted. That said, a resolution of $\Delta\sigma = 0.025$ ($\approx$25 hPa) is still required for reasonable simulation of equilibrium water-vapour profiles, with

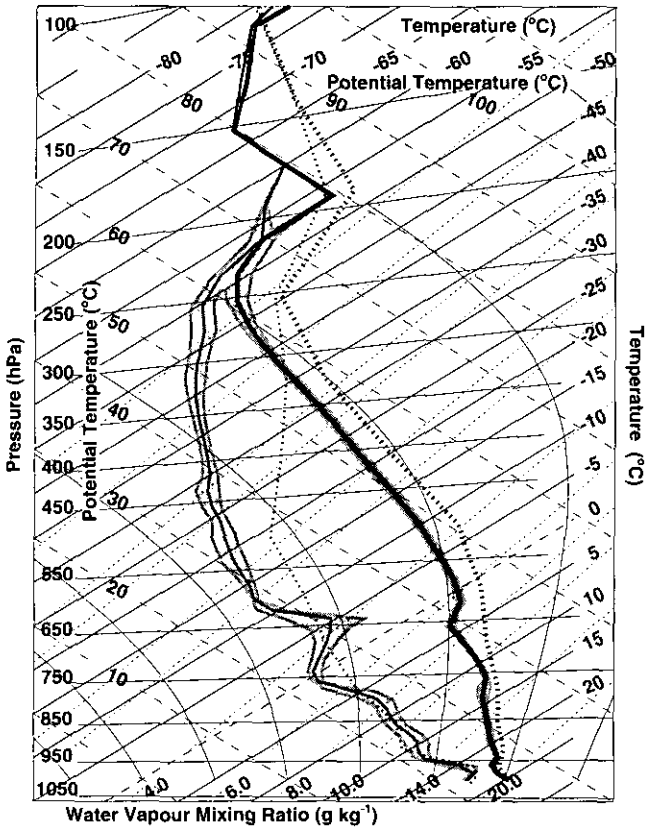

Figure 8. Tephigram plotting equilibrium temperature (thick lines) and dew point (thin lines) for the ECHAM model using the standard 19 layers (dotted lines) and $\Delta\sigma = 0.02$ (solid lines). The shaded area indicates the standard deviation of the $\Delta\sigma = 0.02$ case.

moisture in the $\Delta\sigma = 0.05$ simulation exceeding the converged value by up to 30% in the upper half of the troposphere.

It is also apparent in the temperature profiles of Fig. 9 that the height of the tropopause varies considerably, clearly being lower in altitude in the coarse-resolution cases. When the resolution is fixed at both the top and bottom of the domain (Fig. 10) this is no longer the case. The coarser-resolution experiments are dryer and cooler when the convective detrainment region is well resolved. Thus, improving upper-tropospheric resolution would better reproduce the height of the observed relative-humidity minimum (Fig. 6).

A striking feature in all the experiments is the 'bulge' in the water-vapour structure at 650 hPa that first starts to appear when the layer thickness is less than $\Delta\sigma = 0.033$. Above this height the atmospheric vapour differs substantially with higher vertical resolution. This structure is a direct result of the microphysics parametrizations included in the model's cloud scheme, and is specifically associated with the melting layer of snow. This layer, which is associated with the 'bright band' in radar data, is quite narrow, and was assumed to be around 700 m in depth (approximately 55 hPa) by Kitchen *et al.* (1994). In ECHAM, this layer is under-resolved when resolutions coarser than $\Delta\sigma = 0.025$ are used (i.e. the process occurs at only one grid point). Thus, with increasing vertical resolution the melting of snow and associated cooling are concentrated into a

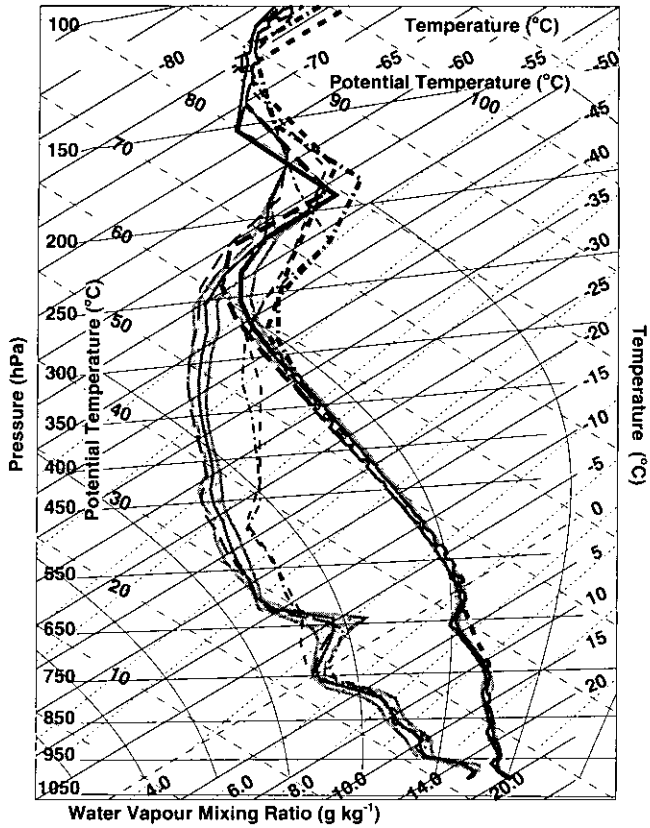

Figure 9. Tephigram plotting equilibrium temperature (thick lines) and dew point (thin lines) for the ECHAM model using a resolution of $\Delta\sigma = 0.05$ (dashed lines), $\Delta\sigma = 0.033$ (dot-dashed lines), $\Delta\sigma = 0.025$ (long dashed lines), $\Delta\sigma = 0.02$ (solid lines), above $\sigma = 0.9$ and a fixed boundary layer (see text for details). The shaded area indicates the standard deviation of the $\Delta\sigma = 0.02$ case.

thinner layer. This has two feedback effects. First, the extra cooling causes a marked change in the stability at this height; this causes deep convection to detrain at this level, and alters the whole mass-flux profile of convection. This is clearly visible when the equilibrium profiles of liquid water detrained from convective updraughts are examined (Fig. 11). With a resolution of $\Delta\sigma = 0.05$ there is no peak at all in detrained water vapour at the melting level. A peak first appears with $\Delta\sigma = 0.033$, which becomes more sharply defined as resolution increases. This has also been observed in tropical observations (Johnson *et al.* 1996). Increasing the detrainment at one height will also affect the mass-flux profile above this level, and significant sensitivity is indeed apparent. However, it is found that the majority of this is due to the changing resolution in the upper atmosphere, and is mostly removed when the atmosphere above 300 hPa is well resolved (Fig. 12).

A second feedback occurs owing to the resolution of the melting layer, since the extra cooling, and the associated increase in humidity due to the increased convective detrainment, is enough to increase relative humidity above 60%. This is the critical threshold at which cloud is assumed to form and thus many cloud processes in the stratiform cloud scheme are initiated.

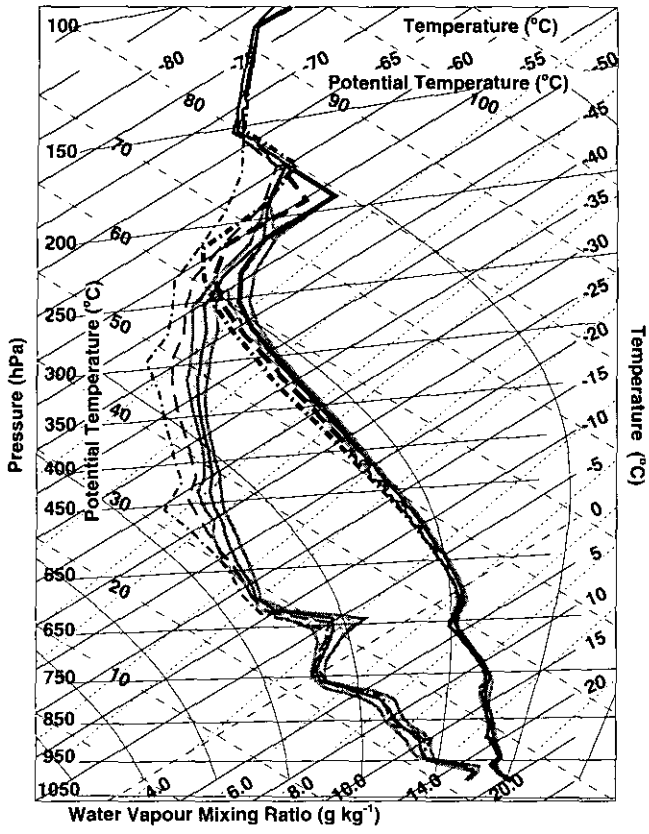

Figure 10. Tephigram plotting equilibrium temperature (thick lines) and dew point (thin lines) for the ECHAM model using a resolution of $\Delta\sigma = 0.033$ (dot-dashed lines), $\Delta\sigma = 0.025$ (long dashed lines), $\Delta\sigma = 0.02$ (solid lines), between $\sigma = 0.9$ and $\sigma = 0.3$ and a fixed resolution otherwise (see text for details). The $\Delta\sigma = 0.05$ case is omitted for clarity. The shaded area indicates the standard deviation of the $\Delta\sigma = 0.02$ case.

(*b*) *EMANUEL model sensitivity*

Figure 13 shows the equilibrium state using the Emanuel model with the same range of tropospheric vertical resolutions. As in the case of the ECHAM model, the atmosphere tends towards a drier state as resolution increases. The general tendency toward moistening with coarser resolution is exactly what one expects with insufficient resolution of a substance that decays exponentially with height. The boundary-layer water-vapour content is constrained so that the bulk surface flux formula gives the flux required to balance the radiative cooling; the moistening above the boundary layer represents the effect of artificial (numerical) diffusion.

The Emanuel model is found to converge at a slower rate than the ECHAM model, with convergence still not fully achieved at $\Delta\sigma = 0.015$. That said, once the resolution exceeds 20 hPa the sensitivity to further increases in resolution is very limited (smaller than the variability of ECHAM). Thus, considering the many uncertainties contained in convective parametrization schemes, convergence can be considered to have been largely achieved in the Emanuel model at an approximate resolution of 20 to 25 hPa, similar to that of the ECHAM model.

In comparison with the water-vapour profile, it is seen that the temperature profile shows almost no sensitivity to vertical resolution degradation, and is tied closely to

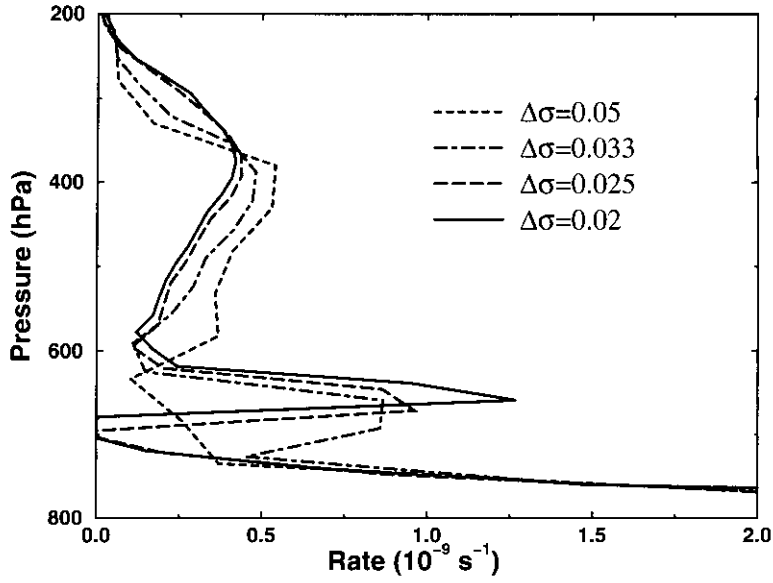

Figure 11. Equilibrium detrainment rate of cloud water from deep convection for the ECHAM case with fixed boundary-layer resolution.

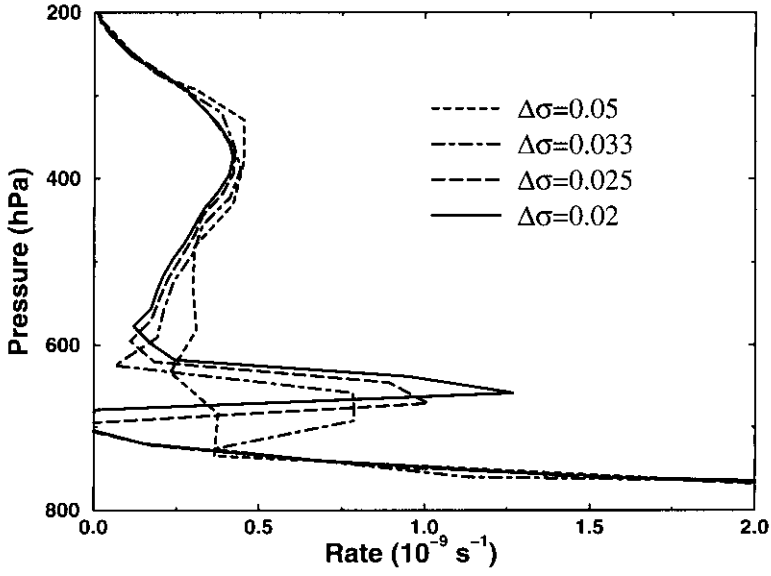

Figure 12. Equilibrium detrainment rate of cloud water from deep convection for the ECHAM case with fixed boundary-layer and upper-tropospheric resolution.

the moist adiabat arising from the model's base level. As was the case for ECHAM, the use of just 10 vertical layers produces vastly different behaviour in the equilibrium state of the upper-tropospheric water vapour (not shown). The Emanuel model is not as sensitive to resolution in the boundary layer, as it uses interpolated values of the levels of free convection and condensation.

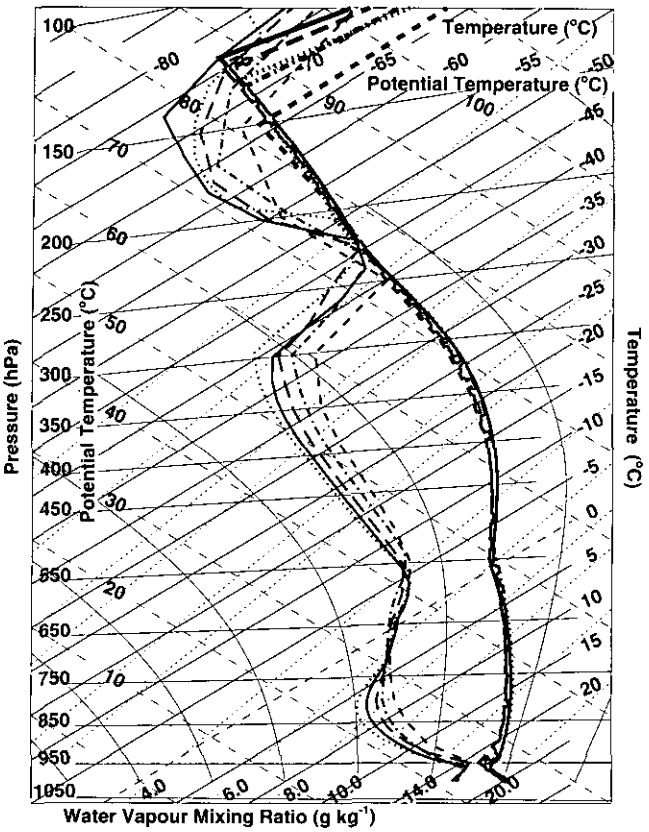

Figure 13. Tephigram plotting equilibrium temperature (thick lines) and dew point (thin lines) for the Emanuel model using a resolution of $\Delta\sigma = 0.05$ (dashed lines), $\Delta\sigma = 0.033$ (dot-dashed lines), $\Delta\sigma = 0.025$ (long dashed lines), $\Delta\sigma = 0.02$ (solid lines), and $\Delta\sigma = 0.015$ (dotted lines) between the surface and 100 hPa, in addition to the 10 fixed layers placed above 100 hPa.

6. Conclusions

In order to achieve high-quality predictions of water vapour using GCMs, it is necessary (but not sufficient) to attain numerical convergence in the simulation of water-vapour distributions. We have attempted to determine a minimum required vertical resolution by examining the effect of vertical resolution on the tropical radiative–convective equilibrium profiles of two single-column models. The models were run to radiative–convective equilibrium, since the differences that can build up in long-term integrations highlight the sensitivities of the water-vapour profile, providing robust comparisons. Both models are able to simulate reasonable temperature and water-vapour (relative humidity) profiles.

Both models showed significant sensitivity to increased vertical resolution, and each was considered to have converged at a uniform vertical resolution of around 20 to 25 hPa. Further tests with the ECHAM model revealed that the variability was markedly reduced when the boundary layer was well resolved; the Emanuel model is much less sensitive to boundary-layer resolution. The upper-atmospheric profiles of temperature and moisture and the tropopause height were also found to be dependent on upper-tropospheric resolution. It therefore seems crucial that the resolution chosen should

allow both the level of free convection and the detrainment level of deep convection to be well defined.

The ECHAM results also highlight another concern related to vertical resolution. Increasing resolution results in the development of elaborate vertical structure in the water-vapour profile that is completely absent in the lower-resolution cases. This was found to be a direct result of the microphysical processes contained in the cloud scheme. Many of these processes are very temperature dependent and are restricted to thin layers. In particular, the melting layer was found to be well resolved only with a resolution of at least $\Delta\sigma = 0.033$ ($\approx$33 hPa) and, as a consequence of resolving this process, much additional convective detrainment occurs at this level, involving additional feedback with other cloud processes. Thus including a complicated and supposedly more accurate representation of cloud and convective processes in a GCM may not yield more accurate assessments of cloud and water-vapour feedbacks than those produced using simpler schemes if both the water-vapour profile and the processes determining it are not adequately resolved.

We note that inadequate resolution of water vapour does not necessarily imply that the water-vapour feedback is incorrectly modelled, but one is entitled to remain sceptical of water-vapour feedback calculated using models with demonstrably insufficient vertical resolution.

Finally, it should be stressed that the 25 hPa convergence limit found in this study only provides a lower bound on the resolution required in GCMs. The inclusion in the full global models of the many processes omitted here, in particular the large-scale horizontal and vertical advection of water vapour, could increase the sensitivity to vertical resolution. Other models, of course, will contain their own set of parametrizations and assumptions, and will have sensitivities that differ from the models selected for this investigation. However, the results shown here emphasize the importance of conducting similar column-model equilibrium tests to ensure that vertical advection and processes contained in increasingly complex parametrization schemes are always well resolved.

ACKNOWLEDGEMENTS

We wish to thank Alex Hall, Pete Inness and an anonymous reviewer for many comments that helped to improve the manuscript, and Robert Colman for information concerning previous resolution studies. Ulrike Lohmann is thanked for much useful discussion that occurred during a visit of the first author to Dalhousie University. During this study Adrian Tompkins was supported by a visiting scientist grant from the Max Planck Society and a European Union Marie Curie Fellowship, FMBICT983005. Kerry Emanuel was supported in part by a grant from the US Department of Energy, DE-FG02-91ER61220.

REFERENCES

Austin, J., Butchart, N. and Swinbank, R. 1997 Sensitivity of ozone and temperature to vertical resolution in a GCM with coupled stratospheric chemistry. *Q. J. R. Meteorol. Soc.*, **123**, 1401–1431

Bacher, A., Obehuber, J. M. and Roeckner, E. 1998 ENSO dynamics and seasonal cycle in the tropical Pacific as simulated by the ECHAM4/OPYC3 coupled general circulation model. *Climate Dyn.*, **14**, 431–450

Betts, A. K. 1990 Greenhouse warming and the tropical water budget. *Bull. Amer. Meteorol. Soc.*, **71**, 1464–1465

Boville, B. A. 1991 Sensitivity of simulated climate to model resolution. *J. Climate*, **4**, 469–485

Boville, B. A. and Randel, W. J. 1992 Equatorial waves in a stratospheric GCM; effects of vertical resolution. *J. Atmos. Sci.*, **49,** 785–801

Brown, R. G. and Bretherton, C. S. 1995 Tropical wave instabilities: Convective interaction with dynamics using the Emanuel convective parameterization. *J. Atmos Sci.*, **52,** 67–82

Chen, C. T. and Roeckner, E. 1996 Validation of the earth radiation budget as simulated by the Max Planck Institute for Meteorology general circulation model ECHAM4 using satellite observations of the Earth Radiation Budget Experiment. *J. Geophys. Res.*, **101,** 4269–4287

1997 Cloud simulations with the Max Planck Institute for Meteorology general circulation model ECHAM4 and comparison with observations. *J. Geophys. Res.*, **102,** 9335–9350

Chen, C. T., Roeckner, E. and Soden, B. J. 1996 A comparison of satellite observations and model simulations of column-integrated moisture and upper-tropospheric humidity. *J. Climate,* **9,** 1561–1585

Chou, M.-D., Krats, D. and Ridgway, W. 1991 Infrared radiation parameterization in numerical models. *J. Climate,* **4,** 424–437

Colman, R. A. and McAvaney, B. J. 1997 A study of the general circulation model climate feedbacks determined from perturbed sea surface temperature experiments. *J. Geophys. Res.*, **102,** 19383–19402

Emanuel, K. A. 1991 A scheme for representing cumulus convection in large-scale models. *J. Atmos. Sci.*, **48,** 2313–2335

1994 *Atmospheric convection.* Oxford University Press

Emanuel, K. A. and Zivkovic-Rothman, M. 1999 Development and evaluation of a convective scheme for use in climate models. *J. Atmos. Sci.*, **56,** 1766–1782

Fowler, L.D., Randall, D. A. and Rutledge, S. A. 1996 Liquid and ice cloud microphysics in the CSU general circulation model. Part I: Model description and simulated cloud microphysical processes. *J. Climate,* **9,** 489–529

Gaffen, D. J., Elliot, W. P. and Robock, A. 1992 Relationships between tropospheric water vapor and surface temperature as observed by radiosondes. *Geophys. Res. Lett.*, **19,** 1839–1842

Ghan, S. J., Leung, L. R. and Hu, Q. 1997 Application of cloud microphysics to the NCAR community climate model. *J. Geophys. Res.*, **102,** 16507–16527

Hansen, J., Ruedy, R., Lacis, A., Russell, G., Sato, M., Lerner, J., Rind, D. and Stone, P. 1997 Wonderland climate model. *J. Geophys. Res.*, **102,** 6823–6830

Johnson, R. H., Ciesielski, P. E. and Hart, K. A. 1996 Tropical inversions near the 0 degree C level. *J. Atmos. Sci.*, **53,** 1838–1855

Kitchen, M., Brown, R. and Davies, A. G. 1994 Real-time correction of weather radar data for the effects of bright band, range and orographic growth in widespread precipitation. *Q. J. R. Meteorol. Soc.*, **120,** 1231–1254

Letreut, H., Li, Z. H. and Forichon, M. 1994 Sensitivity of the LMD general circulation model to greenhouse forcing associated with two different cloud-water parameterizations. *J. Climate,* **7,** 1827–1841

Liao, X. and Rind, D. 1997 Local upper tropospheric/lower stratospheric clear-sky water vapor and tropospheric deep convection. *J. Geophys. Res.*, **102,** 19543–19557

Lindzen, R. S. and Fox-Rabinovitz, M. 1989 Consistent vertical and horizontal resolution. *Mon. Weather Rev.*, **117,** 2575–2583

Lohmann, U. and Feichter, J. 1997 Impact of sulphate aerosols on albedo and lifetime of clouds. *J. Geophys. Res.*, **102,** 13685–13700

Lohmann, U. and Roeckner, E. 1996 Design and performance of a new cloud microphysics scheme developed for the ECHAM general circulation model. *Climate Dyn.*, **12,** 557–572

Manzini, E., McFarlane, N. A. and McLandress, C. 1997 Impact of Doppler spread parameterization on the simulation of the middle atmosphere circulation using the MA/ECHAM4 general circulation model. *J. Geophys. Res.*, **102,** 25751–25762

Marshall, S., Roads, J. O. and Oglesby, R. J. 1997 Effects of resolution and physics on precipitation in the NCAR Community Climate Model. *J. Geophys. Res.*, **102,** 19529–19541

Mitchell, J. F. B., Johns, T. C., Gregory, J. M. and Tett, S. F. B. 1995 Climate response to increasing levels of greenhouse gases and sulphate aerosols. *Nature,* **376,** 501–504

Moron, V., Navarra, A., Ward, M. N. and Roeckner, E. 1998 Skill and reproducibility of seasonal rainfall patterns in the tropics in ECHAM4 GCM simulations with prescribed SST. *Climate Dyn.*, **14,** 83–100

Murphy, J. M. and Mitchell, J. F. B. 1995 Transient response of the Hadley Centre coupled ocean–atmosphere model to increasing carbon-dioxide. 2. Spatial and temporal structure of response. *J. Climate,* **8,** 57–80

Nordeng, T. E. 1994 'Extended versions of the convective parametrization scheme at ECMWF and their impact on the mean and transient activity of the model in the tropics'. ECMWF Technical Report (available from the European Centre for Medium-Range Weather Forecasts, Shinfield Park, Reading, UK)

Olga, P., Persson, G. and Warner, T. T. 1991 Model generation of spurious gravity waves due to inconsistency of the vertical and horizontal resolution. *Mon. Weather Rev.,* **119,** 917–935

Prabhakara, C., Short, D. A. and Vollner, B. E. 1985 El Niño and atmospheric water vapor: Observations from Nimbus 7 SMMR. *J. Climate. Appl. Meteorol.,* **24,** 1311–1324

Raval, A., Oort, A. H. and Ramaswamy, V. 1994 Observed dependence of outgoing longwave radiation on sea surface temperature and moisture. *J. Climate,* **7,** 807–821

Rennó, N. O., Emanuel, K. A. and Stone, P. H. 1994 *Radiative–convective model with an explicit hydrological cycle I:* Formation and sensitivity to model parameters. *J. Geophys. Res.,* **99,** 14429–14441

Rind, D. 1988 Dependence of warm and cold climate depiction on climate model resolution. *J. Climate,* **1,** 965–997

Roekner, E., Arpe, K., Bengtsson, L., Christoph, M., Claussen, M., Dümenil, L., Esch, M., Giorgetta, M. Schlese, U. and Schulzweida, U. 1996 'The atmospheric general circulation model ECHAM4: Model description and simulation of present-day climate'. Technical Report 218, Max Planck Institute for Meteorology, Bundestrasse 55, 20146 Hamburg, Germany

Senior, C. A. 1995 The dependence of climate sensitivity on the horizontal resolution of a GCM. *J. Climate,* **8,** 2860–2880

Senior, C. A. and Mitchell, J. F. B. 1993 Carbon dioxide and climate: The impact of cloud parametrization. *J. Climate,* **6,** 393–418

Slingo, J., Blackburn, M., Betts, A., Brugge, R., Hodges, K., Hoskins, B., Miller, M., Steenman-Clarke, L. and Thuburn, J. 1994 Mean climate and transience in the tropics of the UGAMP GCM: Sensitivity to convective parametrization. *Q. J. R. Meteorol. Soc.,* **120,** 881–922

Sperber, K. R., Hameed, S., Potter, G. L. and Boyle, J. S. 1994 Simulations of the northern summer monsoon in the ECMWF model: Sensitivity to horizontal resolution. *Mon. Weather Rev.,* **122,** 2461–2481

Stephens, G. L. 1990 On the relationship between water vapour over the oceans and sea surface temperature. *J. Climate,* **3,** 634–645

Sun, D. Z. and Lindzen, R. S. 1993 Distribution of tropical tropospheric water vapor. *J. Atmos. Sci.,* **50,** 1643–1660

Teidtke, M. 1989 A comprehensive mass flux scheme for cumulus parameterization in large-scale models. *Mon. Weather Rev.,* **117,** 1779–1800

Tompkins, A. M. and Craig, G. C. 1998a Radiative–convective equilibrium in a three-dimensional cloud ensemble model. *Q. J. R. Meteorol. Soc.,* **124,** 2073–2097

1998b Timescales of adjustment to radiative–convective equilibrium in the tropical atmosphere. *Q. J. R. Meteorol. Soc.,* **124,** 2693–2713

1999 Sensitivity of tropical convection to sea surface temperature in the absence of large-scale flow. *J. Climate,* **12,** 462–476

Weaver, C. P., Collins, W. D. and Grassl, H. 1994 Relationship between clear-sky atmospheric greenhouse effect and deep convection during the Central Equatorial Pacific Experiment: Model calculations and satellite observations. *J. Geophys. Res.,* **99,** 25891–25901

Williamson, D. L., Kiehl, J. T. and Hack, J. J. 1995 Climate sensitivity of the NCAR Community Climate Model (CCM2) to horizontal resolution. *Climate Dyn.,* **11,** 377–397